

Predetermination of Performance Parameters of 3-phase Induction Motor using Numerical Technique Tools

Manjunath B. Ranadev^{1*}, V. R. Sheelavant², R. L. Chakrasali³

¹ Department of Electrical and Electronics Engineering, K.L.E. Institute of Technology, Hubballi, 580 027, Karnataka, India.

¹ mranadev@gmail.com

² Department of Electrical and Electronics Engineering, SDM College of Engineering and Technology, Dharwad, 580 002, Karnataka, India.

² sheel125@gmail.com

³ Department of Electrical and Electronics Engineering, SDM College of Engineering and Technology, Dharwad, 580 002, Karnataka, India.

² pratisatu@yahoo.co.in

Abstract:

The Circle Diagram was used in past for the performance evaluation of 3-phase induction motor under different load conditions. But, now it is not preferred due to availability of programs for detailed analysis. The per-phase equivalent circuit is also not that suitable to estimate the dynamic performance. In this paper, a method is suggested to determine the performance using dq-model. The objective of this paper is to describe modelling in terms of dq variables. The analysis under steady state condition is done using numerical technique tools. The numerical tools such as Gauss-Seidel and Successive Relaxation methods are used and the results are compared with that obtained from the experiment conducted in the laboratory. The comparison of results confirms the validity as well as the accuracy of the proposed methods, as yet another approach to predetermine the performance.

Keywords— iteration, convergence, flux, linkage, performance.

I INTRODUCTION

The squirrel cage type 3- ϕ induction motors are used in industries and have been favoured because of low cost, ruggedness and variable speed options [1]. Though the dynamic model equations are complex but are highly useful in understanding and analyzing the interaction of rotor flux and mmf waves. There are different models available and used based on the reference frame chosen such as stationary, rotor axis, synchronously rotating reference frames. The dq (synchronously rotating) reference frame provides a direct means to obtain the voltage equations to estimate the performance. The dq-model also describes the basic concept of transient modeling and internal fault diagnoses [2, 3]. In dq-model, to establish the required mmf in the air gap the two orthogonal windings are used. Consider two orthogonal windings, one oriented with d-axis and another with q-axis. Because of orthogonal displacement the dq-axis windings are mutually as well as magnetically not coupled. Thus, the current

in dq-windings produce same mmf distribution similar to that of the three phase windings [4].

Over the several years numerical methods are used for providing approximate solutions associated with systems or equations iteratively with the advantage of having high accuracy. The methods used for numerical analysis are listed as direct and iterative. In direct method, a procedure is to be followed with number of steps involved to obtain the solution. An approximate value is assumed and is made to approach towards the accurate solution in iterative method. The merit of iterative method is less memory requirement in computational device. The Gauss-Seidel method is more accurate than other methods and converges quickly. The Successive Relaxation method is employed when the coefficient matrix is symmetric and has a 'property A' and it is a generalization of Gauss-Seidel method [5].

II 3-PHASE INDUCTION MOTOR MATHEMATICAL MODELING

A set of mathematical equations can be used to represent a 3- ϕ induction motor. Consider an arbitrary reference frame, which rotates at a speed of ω_d . Here θ_{da} is the arbitrary angle of dq-winding in regard to stator a-axis. Similarly θ_{dA} is the arbitrary angle of dq-winding set with reference to rotor A-axis is revealed from figure 1.

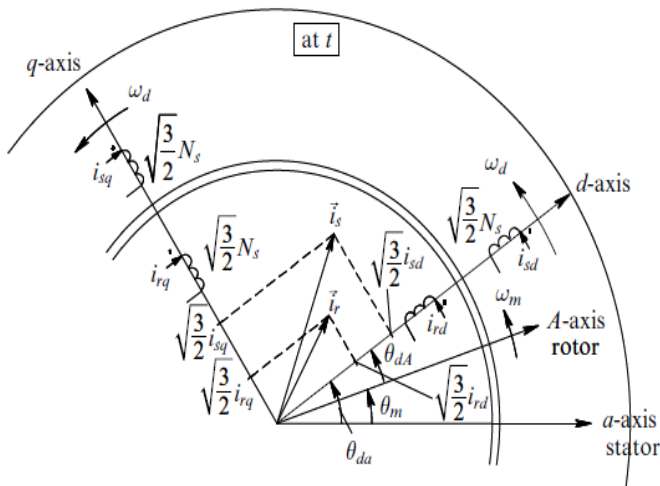


Fig. 1 Stator and rotor dq-windings of 3-phase induction motor

The following notations are used throughout this paper. The rotor dq-winding exhibits a leakage inductance L_{lr} and resistance R_r . Similarly, R_s represent resistance and leakage inductance is represented as L_{ls} of stator dq-winding. The dq-windings of stator and rotor have $\sqrt{3/2} \cdot N_s$ number of turns. Here, N_s depict the number of turns in phase winding of 3-phase induction motor. Because of orthogonal property, there will be magnetic mutual uncoupling between dq-windings. The mutual inductance is zero, because of uncoupling. Thus, L_m represents the magnetizing inductance of dq-winding. Here, P represents total number of poles and p represents derivative operator [6].

The q and d-axis stator current components are represented as i_{sq} and i_{sd} respectively. Similarly i_{rd} and i_{rq} represents dq-axis components of rotor current. The flux linking with either d or q winding is due to current in other winding and that in the same winding. Thus the stator flux linkages in terms of current space vectors are given in equation 1 and 2 [7].

$$\phi_{sd} = L_m \cdot i_{rd} + L_s \cdot i_{sd} \quad (1)$$

$$\phi_{sq} = L_m \cdot i_{rq} + L_s \cdot i_{sq} \quad (2)$$

Similarly, rotor flux linkages in terms of current space vectors are given in equation 3 and 4.

$$\phi_{rd} = L_m \cdot i_{sd} + L_r \cdot i_{rd} \quad (3)$$

$$\phi_{rq} = L_m \cdot i_{sq} + L_r \cdot i_{rq} \quad (4)$$

Where, L_r and L_s exemplify the coefficient of rotor and stator self inductances respectively as mentioned in equation 5.

$$L_s = L_m + L_{ls}, L_r = L_m + L_{lr} \quad (5)$$

Consider an orthogonal set $\alpha\beta$ -winding fixed on the stator. Consider the α -axis in phase with stator winding a-axis. The stator winding voltage is equal to develop the electromotive force to establish the stator flux linkage and to sustain the potential drop in stator resistance. The $\alpha\beta$ -winding voltage equations are stated in 6 and 7.

$$V_{s\alpha} = R_s \cdot i_{s\alpha} + p\phi_{s\alpha} \quad (6)$$

$$V_{s\beta} = R_s \cdot i_{s\beta} + p\phi_{s\beta} \quad (7)$$

The α -axis voltage space vectors are related to the d-axis as given in equation 8.

$$V_{(s,\alpha\beta)} = V_{(s,dq)} e^{j\theta_{da}} \quad (8)$$

Where, $\omega_d = p\theta_{da}$ is the dq-winding speed expressed in electrical radians/ second with regard to stator a-axis speed in air gap. The real component and fictitious component of the dq-winding voltage expressions are given in 9-12.

$$V_{sd} = R_s \cdot i_{sd} - \omega_d \cdot \phi_{sq} + p\phi_{sd} \quad (9)$$

$$V_{sq} = R_s \cdot i_{sq} + \omega_d \cdot \phi_{sd} + p\phi_{sq} \quad (10)$$

$$V_{rd} = R_r \cdot i_{rd} - \omega_{dA} \cdot \phi_{rq} + p\phi_{rd} \quad (11)$$

$$V_{rq} = R_r \cdot i_{rq} + \omega_{dA} \cdot \phi_{rd} + p\phi_{rq} \quad (12)$$

where, $p\theta_{dA} = \omega_{dA}$ is the dq-winding speed expressed in electrical radians/second with regard to the speed of rotor A-axis. Further the voltage expressions in terms of inductances given in 13-16.

$$V_{sd} = L_m \cdot p(i_{sd} + i_{rd}) + R_s \cdot i_{sd} + L_{ls} \cdot p i_{sd} - \omega_d \cdot \phi_{sq} \quad (13)$$

$$V_{sq} = L_m \cdot p(i_{sq} + i_{rq}) + \omega_d \cdot \phi_{sd} + R_s \cdot i_{sq} + L_{ls} \cdot p i_{sq} \quad (14)$$

$$V_{rd} = L_m \cdot p(i_{sd} + i_{rd}) + R_r \cdot i_{rd} + L_{lr} \cdot p i_{rd} - \omega_{dA} \cdot \phi_{rq} \quad (15)$$

$$V_{rq} = L_m \cdot p(i_{sq} + i_{rq}) + \omega_{dA} \cdot \phi_{rd} + R_r \cdot i_{rq} + L_{lr} \cdot p i_{rq} \quad (16)$$

Let $V_{rd} = V_{rq} = 0$, because in squirrel cage motor the rotor conductor are shorted. The above equations explain the 3-phase induction motor dynamic model. The instantaneous reactive power and real power input in terms of dq variables are given in equation 17 and equation 18 [8].

$$Q_{in} = (3/2) \cdot (-V_{sd} \cdot i_{sq} + V_{sq} \cdot i_{sd}) \quad (17)$$

$$P_{in} = (3/2) \cdot (V_{sd} \cdot i_{sd} + V_{sq} \cdot i_{sq}) \quad (18)$$

The output power is given by equation 19.

$$P_{out} = (3/2) \cdot \omega_m \cdot (\phi_{rq} \cdot i_{rd} - \phi_{rd} \cdot i_{rq}) \quad (19)$$

The developed torque obtained is given by equation 20.

$$T_{em} = (3/4) \cdot P \cdot (\phi_{rq} \cdot i_{rd} - \phi_{rd} \cdot i_{rq}) \quad (20)$$



Fig. 2 Experimental setup: 3-phase induction motor coupled with DC shunt machine.

The following are the specifications of DC shunt machine: Power=3 kilo Watts, Voltage=220 Volts, Rated Full-Load Current=15.9 A, Rated Speed=1500 revolutions per minute, Excitation Voltage=220 Volts, Excitation Current=1.02 A, Efficiency=80%.

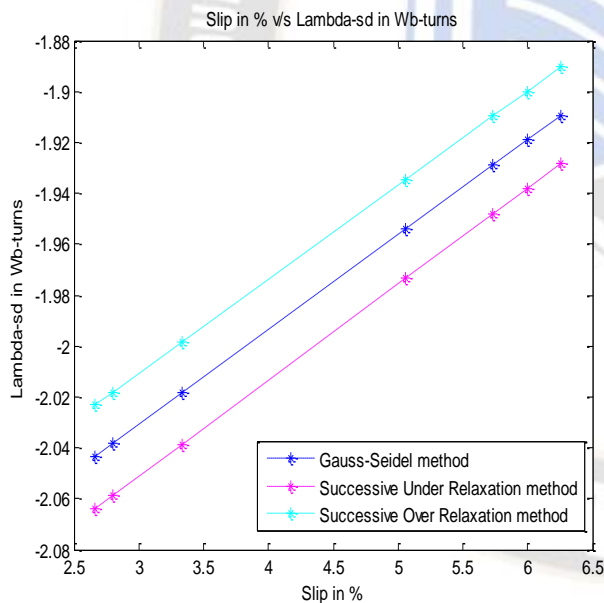


Fig. 3 Slip in % versus stator flux linkages ϕ_{sd} in weber-turns.

It is depicted from figure 3 that ϕ_{sd} increases with increase in slip. It is because i) stator self inductance is assertive ii) as slip increases i_{sd} increases and i_{rd} decreases. Hence, as slip increases ϕ_{sd} increases. The value of ϕ_{sd} obtained at 6.26% slip is -1.9093 Wb-turns using Gauss-Seidel method and it is -1.8903 Wb-turns and -1.9285Wb-turns using Successive Over-Relaxation method and Successive Under -Relaxation method respectively.

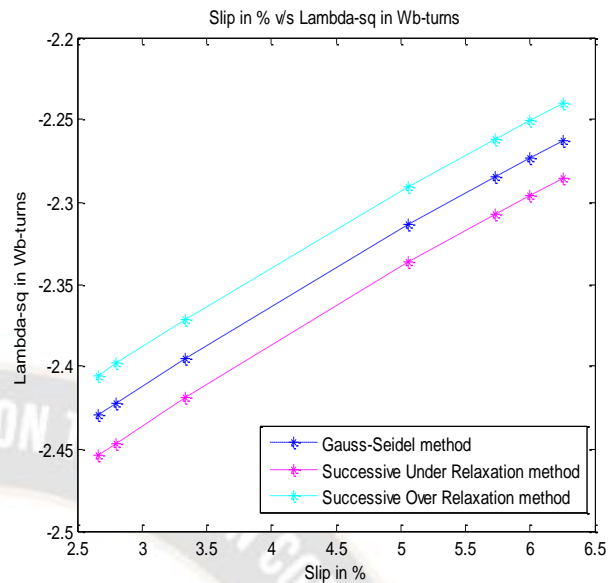


Fig. 4 Slip in % versus stator flux linkages ϕ_{sq} in weber-turns.

Similarly as slip increases i_{sq} decreases and i_{rq} increases. Hence ϕ_{sq} increases with slip as shown in figure 4.

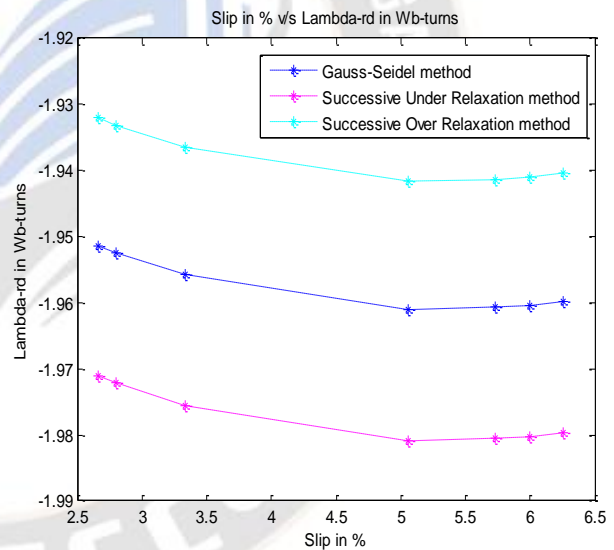


Fig. 5 Slip in % versus rotor flux linkages ϕ_{rd} in weber-turns.

It is depicted from figure 5 that ϕ_{rd} decreases w.r.t. increase in slip. It is because i) the influence of rotor self inductance ii) as slip increases i_{rd} decreases and i_{sd} increases. Hence, as slip increases ϕ_{rd} decreases. The value of ϕ_{rd} obtained at 6.26% slip is -1.9598 Wb-turns using Gauss-Seidel method and it is -1.9404 Wb-turns and -1.9796 Wb-turns using Successive Over-Relaxation method and Successive Under-Relaxation method respectively.

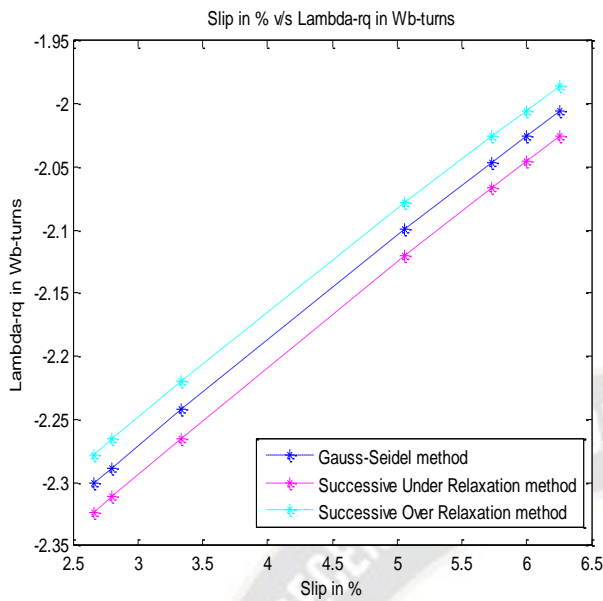


Fig. 6 Slip in % versus rotor flux linkages ϕ_{rq} in weber-turns.

Similarly as slip increases i_{rq} increases and i_{sq} decreases. Hence ϕ_{rq} increases with slip as shown in figure 6.

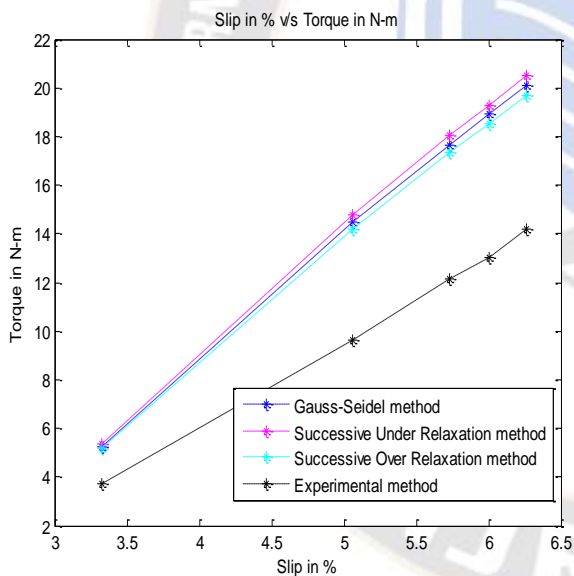


Fig. 7 Slip versus torque characteristics

As shown in figure 7, torque increases with increase in slip. It is because of decrease in ϕ_{rd} and increase in ϕ_{rq} . Hence the difference increases and torque increases with slip. This is given in equation 20. The value of torque obtained at 6.26% slip is 20.08 N-m using Gauss-Seidel method. The value of torque at full load obtained using Successive Under-Relaxation and Over-Relaxation method are 20.49 N-m and 19.69 N-m respectively. The torque obtained at 6.26% slip by experimental method is 14.20 N-m. The difference is assumed to be associated with meters accuracy, reading accuracy and dynamics of machine in real time condition.

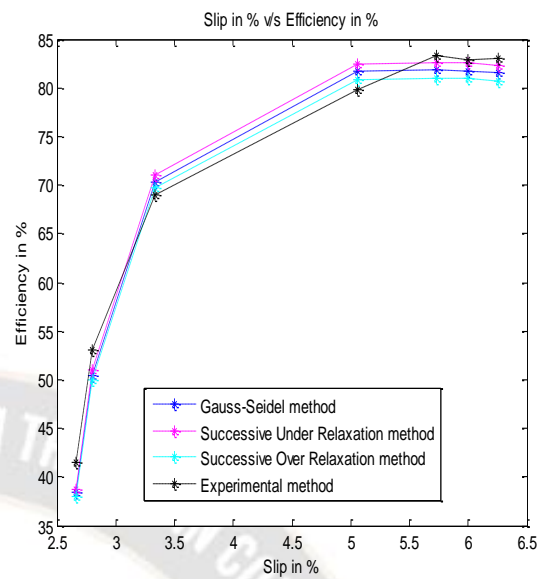


Fig. 8 Slip in % versus efficiency in %.

The efficiency obtained at 6.26% slip is 81.53% using Gauss-Seidel method. The efficiency at 6.26% slip using Successive Under-Relaxation and Over-Relaxation method are 82.35% and 80.72 % respectively. The efficiency obtained from experimental test at 6.26% slip is 82.97%. The obtained efficiency by Gauss-Seidel and Relaxation methods are comparable with the experimental method and are within the acceptable range as shown in figure 8.

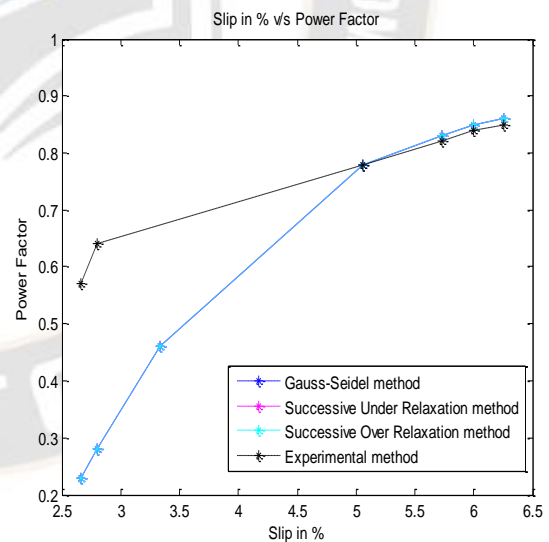


Fig. 9 Slip in % versus power factor.

The power factor obtained at 6.26% slip is 0.86 using Gauss-Seidel method and both Relaxation methods. The obtained value of power factor from the experimental method at 6.26% slip is 0.85. The power factor obtained by both Gauss-Seidel method and relaxation methods are analogous with the experimental method. The power factor variation with slip is shown in figure 9. The machine, when running at 3/4th to full load exhibit good power factor.

4.1 Comparison of the results with the published work:

The Gauss-Seidel method and both Relaxation methods require calculation of first-order derivative. The number of calculations increases with the order of the equations also increases the simulation time. The Gauss-Seidel method and both Relaxation methods took almost same number of steps and comparable with existing methods. The step size that provides 10% relative error for different methods is summarized as shown in figure 10 [10].

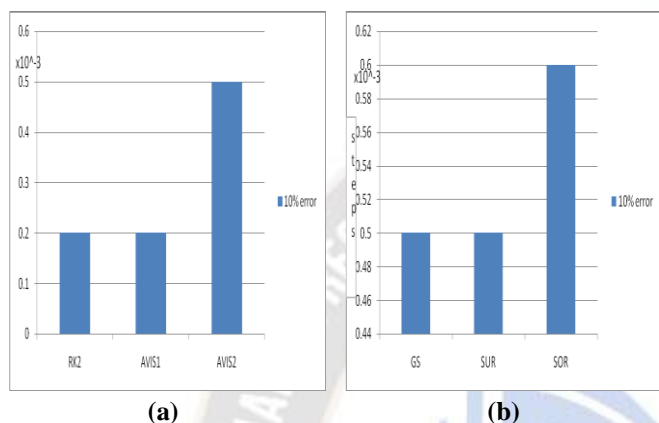


Fig. 10 Comparison of steps for 10% relative error (a) existing methods (b) proposed methods.

RK2: Second-order Runge–Kutta, AVIS2: Average Voltage at the Integration Step

The results obtained from no-load, locked rotor and dc resistance test are as follows. The change in efficiency observed is 14.6% from no load to full load. The highest power factor obtained is 0.686 [11]. The above results are compared with the results obtained from both Relaxation and Gauss-Seidel methods. The change in efficiency is 15% to 20% from no load to full load. The highest value of power factor obtained is 0.86.

V CONCLUSION

The dynamic model is developed and the mathematical model is presented for a 3-φ induction motor. The numerical technique tools are used to study the behaviour. It is observed that there is a close matching between the results obtained from the Successive Relaxation methods, Gauss-Seidel method and the experimental method. Thus proves the validity of numerical methods for analysing the steady state behaviour. The use of numerical methods, reduce the computational overheads while analysing the steady-state behaviour. It is evident that as slip increases the power factor of the motor increases. Thus, the input current increases and addresses also power quality related issues.

REFERENCES:

[1]. L.A. Pereira, M. Perin, L.F.A. Pereira et al., “ Performance estimation of three-phase induction motors from no-load

startup test without speed Acquisition”, ISA Transactions, 2019. DOI: 10.1016/j.isatra.2019.05.028.

[2]. Edgar Chulines, Marco A. Rodríguez, Iván Duran, Rafael Sánchez, “Simplified Model of a Three-Phase Induction Motor for Fault Diagnostic Using the Synchronous Reference Frame DQ and Parity Equations”, ScienceDirect IFAC Papers OnLine, pp. 662–667, 2018. DOI: 10.1016/j.ifacol.2018.07.356.

[3]. Nouby M. Ghazaly, A. H. H. . (2022). A Review of Using Natural Gas in Internal Combustion Engines. International Journal on Recent Technologies in Mechanical and Electrical Engineering, 9(2), 07–12. <https://doi.org/10.17762/ijrme.v9i2.365>

[4]. Bindu, S., & Thomas, V. V., “Characteristic signature identification of air-gap eccentricity faults using extended d-q model for three phase induction motor”, International Conference on Condition Assessment Techniques in Electrical Systems, CATCON 2015, pp. 157-162, 2016. DOI: 10.1109/CATCON.2015.7449526.

[5]. Chaudhary, D. S. . (2022). Analysis of Concept of Big Data Process, Strategies, Adoption and Implementation. International Journal on Future Revolution in Computer Science & Communication Engineering, 8(1), 05–08. <https://doi.org/10.17762/ijfrcsce.v8i1.2065>

[6]. C. Kalaivani, K. Rajambal, “Dynamic Modeling of Seven-Phase Induction Generator”, ScienceDirect, Energy Procedia 117, pp. 369–376, 2017.

[7]. A. Sternecki, O. Biro, K. Preis, S. Rainer, G. Ofner, “Numerical analysis of steady-state operation of three-phase induction machines by an approximate frequency domain technique”, Elektro technik & Information stechnik, vol 128, issue 3, pp. 81-85, 2011.

[8]. Ned Mohan, “Advanced Electric Drives- Analysis, Control and Modeling using MATLAB/Simulink”, Wiley & Sons, Inc., Hoboken, New Jersey, 2014.

[9]. Pratik Anil Ghive, “Dynamic Modeling of Induction Motor for EV”, International Journal For Technological Research in Engineering, Volume 5, Issue 9, pp. 3880-3884, May-2018.

[10]. E. T. Nekerow, D. Yakob, and D. Teshome, “Data mining based medical intelligent system for chronic kidney disease diagnosis and treatment in the Oromo language”, Int J Intell Syst Appl Eng, vol. 10, no. 2, pp. 232–241, May 2022.

[11]. Dal Y. Ohm, “Dynamic Model of Induction Motors for Vector Control”, Drivetech, Inc., Blacksburg, Virginia.

[12]. M K Jain, S R K Iyengar, R K Jain, “Numerical Methods for Scientific and Engineering Computation”, New Age International (P) Limited, 2007.

[13]. Oleksiy Kuznyetsov, “Mathematical Model of a Three-Phase Induction Machine in a Natural Reference Frame Utilizing the Method of Numerical Integration of Average Voltages at the Integration Step and Its Application to the Analysis of Electromechanical Systems”, Mathematical Problems in Engineering, Volume 2019, Article ID 4581769, 13 pages.

[14]. Mohamed Samir, Dr. Gagan Singh, Nafees Ahmed, Husain Ahmed, “Dynamic Performance Analysis of Three Phase Induction Motor with Single Phasing”, Conference on

Advances in Communication and Control Systems 2013 (CAC2S 2013), Atlantis Press, pp. 216-221, 2013.

- [15]. Kashif Ali Abro1, Abdon Atangana, "Numerical and mathematical analysis of induction motor by means of AB–fractal–fractional differentiation actuated by drilling system", Wiley Periodicals LLC, pp. 1-15, October 2020.
- [16]. G. Sharma, D. Parashar and A. Chandel, "Analysis of Dynamic Model of Three Phase Induction Motor with MATLAB/SIMULINK," 2020 *International Conference on Advances in Computing, Communication & Materials (ICACCM)*, pp. 51-58, 2020.

